HHS Public Access

Author manuscript

Biochemistry. Author manuscript; available in PMC 2021 May 12.

Published in final edited form as:

Biochemistry. 2020 May 12; 59(18): 1728–1736. doi:10.1021/acs.biochem.0c00080.

Inhibition of Excision of Oxidatively Generated Hydantoin DNA Lesions by NEIL1 by the Competitive Binding of the Nucleotide Excision Repair Factor XPC-RAD23B

Marina Kolbanovskiy[1], **Yoonjung Shim**[2], **Jung-Hyun Min**[3], **Nicholas E. Geacintov**[1], **Vladimir Shafirovich**[*,1]

[1]Chemistry Department, New York University, 31 Washington Place, New York, NY 10003-5180, United States

[2]Department of Chemistry, University of Illinois at Chicago, Chicago, IL 60607, United States

[3]Department of Chemistry and Biochemistry, Baylor University, Waco, TX 76798, United States

Abstract

The interplay between nucleotide excision repair (NER) and base excision repair (BER) of non-bulky, oxidatively generated DNA lesion, has long been a subject of significant interest. The hydantoin oxidation products of 8-oxoguanine, spiroiminodihydantoin (Sp) and 5-guanidinohydantoin (Gh), are substrates of both BER and NER in HeLa cell extracts and human cells [Shafirovich et al. (2019) *Chem. Res. Toxicol. 32,* 753–761]. The primary factor that recognizes DNA lesions is the DNA damage-sensing factor XPC-RAD23B (XPC), while the glycosylase NEIL1 is known to remove Gh and Sp lesions from double-stranded DNA. It is shown here that in aqueous solutions containing nanomolar concentrations of proteins, XPC and NEIL1 compete for binding to 147-mer oligonucleotide duplexes that contain single Gh or Sp lesions under conditions of [protein] >> [DNA] concentrations, thus inhibiting the rate of BER catalysed by NEIL1. The non-covalently bound NEIL1 molecules can be displaced by XPC at concentration ratios R = [XPC]/[NEIL1] > 0.2, while full displacement of NEIL1 is observed at $R \geq 0.5$. In the absence of XPC and under single turnover conditions, only the burst phase is observable. However, upon progressively increasing the XPC concentration, the amplitude of the burst phase decreases gradually, and a slower time-dependent phase of incision product formation manifests itself with rate constants of 3.0×10^{-3} (Gh) and 0.90×10^{-3} s^{-1} (Sp). These slow kinetics are attributed to the dissociation of XPC-DNA complexes that allow for the rebinding of NEIL1 to the temporarily exposed Gh or Sp lesions, and the incisions observed under these steady-state conditions.

[*]**Corresponding Author:** V. Shafirovich, vs5@nyu.edu, Tel: (212) 998-8456, FAX : (212) 995-4205.

The authors declare no competing financial interest.

ASSOCIATED CONTENT

Supporting Information

Figure S1 shows that the NEIL1-SpDNA and $(NEIL)_2$ – SpDNA complexes (Figure 1B) are almost fully incised and contain the 65 nt NEIL1 incision products. Figure S2 illustrates the *Log(mobility)* vs. *Log(Mass)* relationship. Figure S3 shows simulated incision product formation of GhDNA product formation induced by NEIL1 with and without unmodified DNA, while Figure S4 depicts the simulated effects of unmodified DNA on burst phase kinetics of GhDNA incised by NEIL1 (effects of the k_N values on the burst phase kinetics incisions at constant k_X/k_N ratios and relationship between of umDNA/NEIL1 ratios at different k_{umD}/k_N ratios on the reciprocal burst phase amplitudes). This material is available free of charge on the ACS Publications website.

Graphical Abstract

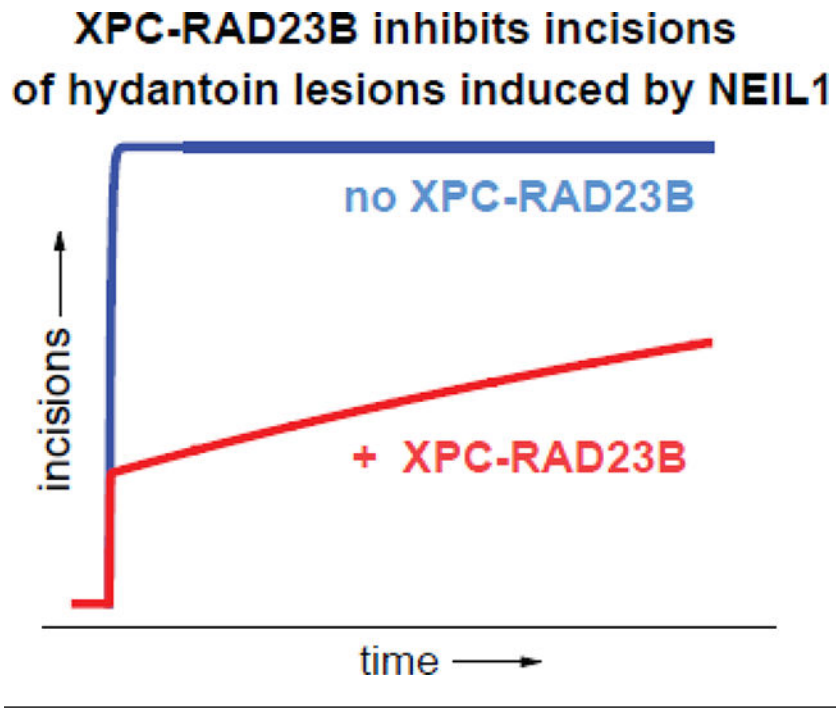

INTRODUCTION

The repair of oxidatively generated DNA lesions is a crucial factor for maintaining genomic stability during oxidative stress.[1] In general, non-bulky oxidatively generated DNA lesions are removed by base excision repair (BER) mechanisms, while bulky DNA double helix-distorting lesions are excised by nucleotide excision repair (NER) machinery.[2–5] Oxidatively generated DNA damage targets guanine,[6] the most easily oxidizable natural nucleic acid base.[7] Sequential oxidation of guanine generates a series of guanine modifications including the well-known 8-oxo-7,8-dihydroguanine (8-oxoG),[6] and further oxidation products of 8-oxoG, such as the diastereomeric spiroiminodihydantoin (Sp) and 5-guanidinohydantoin (Gh) (Figure 1).[8]

Although the cellular levels of hydantoin lesions are low,[9] these lesions can contribute to the malignant transformations of cells because they are at least one order of magnitude more mutagenic than 8-oxoG.[10]

Hydantoin lesions are excellent substrates of BER enzymes that include glycosylases NEIL1 and NEIL3.[11–14] Human NEIL1 is a bifunctional DNA glycosylase that cleaves the N-glycosyl bond of the hydantoin lesions and excises the resulting abasic site by a lyase β,δ elimination mechanism that results in 3′ and 5′ phosphate ends at the cleavage site.[15–17]

The possible interplay between different repair pathways such as BER and NER in removing oxidatively generated DNA lesions from double-stranded DNA has been of significant interest for some time.[18–20] Recently, we found that hydantoin lesions are excised by NER and BER pathways in human cell-free extracts[21] and in intact human cells.[22] However, it

remained unclear how these two repair pathways compete with one another in the excision of the same DNA lesions in biological systems.

In this work, we demonstrate that the heterodimeric DNA damage-sensing NER factor XPC-RAD23B (XPC) competes with the BER enzyme NEIL1 for binding to the same Gh and Sp hydantoin lesions embedded 147 base pair (bp), ^{32}P-internally labeled double-stranded DNA substrates (Figure 1). The formation of NEIL1- and XPC-RAD23B-DNA complexes was monitored by electrophoretic mobility shift assays (EMSA).[23] The kinetics of the glycosylase/lyase activity of NEIL1 in the presence of XPC-RAD23B was monitored by the formation of the ^{32}P-labeled DNA fragments derived from the DNA strand cleavage at the lesion site. Numerical least-squares fitting routines of the BER-induced product yields as a function of reaction time using the DynaFit4 software package,[24] allowed us to estimate the dissociation rate constant of XPC from non-covalent XPC-DNA complexes by monitoring the binding and subsequent cleavage of the DNA strands by NEIL1.

MATERIALS AND METHODS

Construction of 147 bp DNA Substrates

The 2'-oligodeoxynucleotides were purchased from Integrated DNA Technologies (Coralville, IA, USA) and purified by denaturing polyacrylamide gel electrophoresis. The 11-mer oligonucleotide adducts containing the *S*-Sp and *R*-Sp diastereomers were generated by the site-selective oxidation of guanine in the 5'-CCATCGCTACC sequence using photochemically generated carbonate radical anions at pH 7.5 – 8.0 to oxidize the guanine residue as described earlier.[25–27] The Gh-modified oligonucleotides were prepared by the oxidation of 5'-CCATC[8-oxoG]CTACC sequences with $(NH_4)_2IrCl_6$ complex at pH 6.0.[8, 28] The Sp or Gh modified oligonucleotides were isolated and purified by anion-exchange HPLC.[28, 29] The Sp adduct containing the *S*-Sp diastereomer was the first-eluting fraction (Sp1), whereas the Sp oligonucleotide with the *R*-Sp diastereomer eluted in the second fraction (Sp2) on a DNAPac PA-100 column (Dionex, Sunnyvale, CA, USA).[30]

The 147 bp DNA duplexes were equivalent to the Widom 601 DNA sequence,[31] except for the 11-mer fragment containing the single site-specific hydantoin lesion (Figure 1). These 11-mers were inserted into 147-mer sequences by replacing an equal number of the parent nucleotides so that the lesions were positioned at the 66th nucleotide counted from the 5′-end of the 147-mer (Figure 1). The 147-mer modified strands were assembled by ligating the 5′–^{32}P-labeled 11-mers 5′-CCATCHCTACC (H = *S*-Sp, Gh, or G) to the 5′-and the 3′-flanking 60- and 76-mer sequences, 5′-CACAGGATGTATATATCTGACACGTGCCTGGAGACTAGGGAGTAATCCCCTTGGCGGTTA, and 5′-ACAGCGCGTACGTGCGTTTAAGCGGTGCTAGAGCTGTCTACGACCAATTGAGCGGCCTCGGCACCGGGATTCTCCA, respectively.[32] The 147-mer modified sequences obtained by this approach were purified by denaturing PAGE and annealed with their complementary strands (bearing C-bases opposite the lesion, Figure 1) by heating at 90 °C for 5 min, followed by a slow cooling to room temperature overnight to form the 147 bp DNA duplexes.

XPC-RAD23B and NEIL1

Human NEIL1 protein was expressed in *Escherichia coli* cells and purified as described elsewhere.[33] The NEIL1 samples were provided by R. Steven Lloyd (Oregon Health and Science University). Human His-XPC-RAD23B (full length) was overexpressed and purified from insect cells as described previously.[34] The purified proteins were stored at −78 °C. The concentrations of the proteins were determined by the Bradford assay using bovine serum albumin (BSA) as the standard. Active site titrations[12, 35] of XPC-RAD23B or NEIL1 were performed using 20 nM 147bp SpDNA duplexes spiked with traces of ^{32}P-internally labeled SpDNA, and all concentrations of XPC-RAD23B or NEIL1 obtained from the analysis of either native (XPC-RAD23B) or denaturing (NEIL1) gels are given as active concentrations.

EMSA Assays

The binding of proteins to 147 bp double-stranded DNA substrates was investigated in 20 μL binding buffer (20 mM sodium phosphate, pH 7.4, 5 mM $MgCl_2$, 1 mM EDTA, 150 mM NaCl, 1 mM dithiothreitol, 5% glycerol, 0.01% Triton X-100, 100 ng/μL BSA, 5 ng/μL) after incubation for 5 – 10 min at 25 °C. These solutions contained 0.1 nM ^{32}P-labeled DNA substrate, and the indicated concentrations of NEIL1 and/or XPC-RAD23B proteins, 5 ng/μL covalently closed circular pBR322 plasmid) containing 0.1 nM ^{32}P-labeled DNA substrate.[36] The samples were then placed on ice and aliquots of the reaction mixtures were loaded onto 5% non-denaturing polyacrylamide gels (acrylamine: bisacrylamide, 37.5:1) containing 2.5% glycerol and 1×TBE buffer, and electrophoresed at 7V/cm in a cold room (4 °C).

Glycosylase/Lyase Assay

The glycosylase/lyase activity of NEIL1 protein was evaluated in 100 μL buffer (20 mM sodium phosphate, pH 7.4; 5 mM $MgCl_2$, 1 mM EDTA, 150 mM NaCl, 1 mM dithiothreitol, 5% glycerol, 0.01% Triton X-100, 100 ng/μL BSA) containing 0.1 nM ^{32}P-internally labeled DNA substrate, the indicated concentrations of NEIL1 and XPC-RAD23B. Aliquots of the reaction mixtures were remove at fixed periods of time (5 s to 30 min) and quenched by the addition of 5 μL of denaturing loading buffer (80% formamide, 0.025% xylene cyanol, 0.025% bromphenol blue in 1×TBE buffer). The samples were then subjected to gel electrophoresis using 12% denaturing polyacrylamide gels in 1×TBE buffer for 2 h.

Analysis of Gel Images

The gels were dried, exposed to Molecular Dynamics Storage Phosphor Screens, and then scanned with a Typhoon FLA 9000 laser scanner. The gel autoradiographs were analysed using Total Lab TL120 1D software. The kinetic parameters (rates constants and their ratios) were obtained from the least-squares fits of the kinetic equations to the experimental data points using the DynaFit4 software package.[24]

RESULTS AND DISCUSSION

Competitive Binding of XPC-RAD23B and NEIL1 Proteins to Hydantoin Lesions

The binding of NEIL1 and XPC-RAD23B proteins to 147 bp ^{32}P-internally labeled DNA duplexes containing single site-specifically positioned Sp and Gh lesions was monitored by standard EMSA methods.[23] Complexes of XPC-RAD23B and NEIL1 with DNA substrates can be easily resolved since the molecular weights of XPC-RAD23B and NEIL1 are 151.1[34] and 43.7 kDa,[17] respectively.

Titrations of the 147 bp DNA substrates with single Sp or Gh lesions by XPC-RAD23B and NEIL1 proteins were performed in the presence of circular covalently closed pBR322 plasmid used as nonspecific competitor DNA[23] in order to minimize the formation of multiple XPC-DNA[34] and NEIL1-DNA[37] complexes. Figure 2 shows the ranges of NEIL1 and XPC protein concentrations that exhibit competitive binding phenomena. Typical autoradiographs of native gels demonstrate that addition of XPC-RAD23B (Figure 2A) or NEIL1 (Figure 2B) to 147 bp ^{32}P-internally labeled SpDNA duplexes result in the appearance of bands due to protein-DNA complexes that migrate more slowly than free Sp-modified DNA molecules.

The highest mobility protein-DNA complexes correspond to either one XPC-RAD23B molecule (XPC-SpDNA, Figure 2A) or one NEIL1 molecule (NEIL1-SpDNA, Figure 2B) bound per DNA molecule that are observed at the lower protein-concentration ranges. At the higher XPC concentrations, slower migrating and weaker intensity bands are observed that are attributed to dimeric $(XPC)_2$-SpDNA complexes[34] (lanes 6, 7, Figure 2A). In the case of NEIL1, formation of the DNA complexes with two NEIL1 molecules $(NEIL1)_2$-SpDNA has also been previously reported[37] and occurs at lower protein concentration (Figure 2B, lanes 3 – 7).

In contrast to XPC, which reversibly binds to SpDNA, the binding of NEIL1 to its substrates is not reversible since NEIL1 promptly catalyzes the incision of the DNA strands at the site of the lesions via its glycosylase/lyase activity.[12] To verify this conclusion, the NEIL1-SpDNA and $(NEIL\ 1)_2$-SpDNA bands were excised from a native gel (Figure S1A in Supporting Information), and the ^{32}P-labeled DNA was recovered. Analysis of these oligonucleotides strands by denaturing PAGE demonstrated that the Sp-modified strands are cleaved by NEIL1, resulting in the formation of 65 nt cleavage fragments as shown in Figure S1B in Supporting Information. Thus, the NEIL1 ^{32}P-labeled complexes resolved by native gel EMSA methods contain DNA duplexes in which the Sp lesion-bearing strands are incised by the NEIL1 glycosylase/lyase activity.

Based on fundamental principles, the relationship between the electrophoretic mobilities μ_M of charged particles and their molar mass M, $\mu_M \propto M^S$, was derived,[38] where S is a theoretical parameter with a value between 1/3 and 2/3. The corresponding linearized form of this relationship, $Log(\mu_M) \propto S \times Log(M)$ can be successfully employed to estimate molar masses of certain protein-DNA complexes from gel electrophoresis experiments.[23] In order to verify that the $(XPC)_2$-SpDNA and $(NEIL1)_2$-SpDNA) complexes truly contain two protein molecules each, we plotted the $Log(\mu_M)$ values (deduced from Figures 2A and 2B)

of all four protein duplexes (XPC-SpDNA, $(XPC)_2$-SpDNA, NEIL1-SpDNA, $(NEIL1)_2$-SpDNA) as a function of *Log(M)*. As shown in Supporting Information (Figure S2), the excellent fit of all four data points to the same straight line is consistent with the assignments of the monomeric and dimeric protein - DNA complexes shown in Figure 2.

The formation of protein-DNA complexes at different proportions of NEIL1 and XPC in pre-formed solutions of these proteins is depicted in Figures 2C and 2D. At a constant [NEIL1] = 3.8 nM concentration and variable XPC concentrations (0.4 nM to 7.8 nM), NEIL1-SpDNA complexes are dominant in the lower range of XPC concentrations in the case of [XPC]/[NEIL1] = 0.1 (Figure 2C, lane 2). At [XPC]/[NEIL1] concentration ratios of 0.2 – 0.5, the NEIL1 protein is gradually displaced by XPC (lanes 3 – 5) and minor traces are observed at the higher ratios (lanes 7 and 8, Figure 2C). Similar results were obtained in the experiments with 147 bp ^{32}P-internally labeled GhDNA in pre-formed NEIL1 and XPC-RAD23B solutions at constant [XPC] = 4.0 nM and [XPC] = 0.2 – 6.3 nM (Figure 2D).

In summary, non-denaturing gel electrophoresis analysis reveals that XPC-RAD23B and NEIL1 proteins bind competitively to DNA duplexes that harbor hydantoin lesions to form non-covalent complexes either with intact damaged DNA (in the case of XPC-RAD23B) or with the product duplexes, in which the lesions were excised by NEIL1 glycosylase/lyase activities. In the next section, employing denaturing gel electrophoresis analysis, we demonstrate that non-covalent binding to XPC-RAD23B inhibit the BER activity of NEIL1.

Inhibition of NEIL1 BER activity by XPC-RAD23B

Aliquots of pre-formed solutions of NEIL1 and XPC-RAD23B were added to solutions of ^{32}P-internally labeled 147-mer DNA duplexes with single Sp lesions, or unmodified 147-mer control duplexes containing guanine instead of Sp. Since NEIL1 is a bifunctional glycosylase, it excises the hydantoin lesions and subsequently cleaves the incised strand via its lyase activity.[12] After incubation of solutions containing NEIL1 and hydantoin-DNA substrates, the reactions were terminated by adding a denaturating loading buffer.[12] The fractions of incisions were monitored by denaturing PAGE methods. Typical autoradiographs of denaturing gels showing the reaction products detected after incubation of 147 bp ^{32}P-internally GhDNA duplexes with NEIL1, are shown in Figure 3A.

Under single-turnover conditions ([NEIL1] >> [GhDNA or SpDNA]), double incisions of the GhDNA strands and the formation of 65 nt oligonucleotide cleavage products, are observed within 5 – 10 s after adding NEIL1 (Figure 3A). The kinetics of NEIL1 – induced incisions of GhDNA and SpDNA strands catalysed by NEIL1 are shown in Figure 4A.

As expected, only the burst phase is evident (yield of cleavage products > 95%) in the case of single turnover conditions ([NEIL1 >> [DNA])[12] (Figure 4A). In the presence of nanomolar concentrations of XPC, the amplitude of the burst phase is reduced to ~ 25 – 50%, depending on the XPC concentration (Figures 4B, C).

In the case of SpDNA duplexes, addition of 4.8 nM XPC reduces the burst phase amplitude to ~62% (Figure 5), while in the case of GhDNA the burst phase is reduced to ~53% under similar conditions (Figure 4B).

Overall, these results can be understood in terms of a competitive binding of XPC and NEIL1 to the same DNA lesions, and the inhibition of NEIL1-catalysed incisions by the non-covalent binding of XPC to the SpDNA and XPC-GhDNA molecules.

The general mechanism of excisions of hydantoin lesions catalysed by NEIL1 was extensively investigated by Krishnamurthy et al. based on Scheme 1:[12]

This mechanism includes the following steps: substrate binding to form non-covalent complexes (rate constants k_1, k_{-1}), cleavage of the glycosidic bond with the formation of an apurinic site (k_G), cleavage of the apurinic site by the NEIL1 lyase activity (k_L), and release of NEIL1 from the product P (k_3) thus completing the enzymatic cycle.[35] The slow escape of the protein from the product complex is typical for BER enzymes, for instance, adenine glycosylase MutY.[35]

In the case of Sp and Gh hydantoin lesions (H in HDNA, Scheme 1), the lyase activity of NEIL1 is very high and the formation of cleavage products can be considered as a one-step reaction with the observed catalytic rate constant, k_2.[12] Experiments under single-turnover conditions ([NEIL1] >> [HDNA]) and high [NEIL1] ~ 400 nM showed that the strand cleavage by the combined glycosylase/lyase activities becomes a rate-determining step; in DNA duplexes containing C opposite *S*-Sp and Gh, the values of k_2 are equal to 3.0 and 2.3 s^{-1}, respectively.[12]

In our single-turnover experiments at NEIL1 concentrations of ~ 5 nM and DNA substrate concentrations of 0.1 nM, the strand cleavage kinetics can be described by a pseudo-second order rate constant (frequently called a specificity constant), $k_N = k_1k_2/(k_{-1} + k_2) = k_2/K_m$, where K_m is the Michaelis constant, $K_m = (k_{-1} + k_2)/k_1$.[35] However, only two parameters (k_2, K_m) among the three (k_1, k_{-1}, and k_2) can be unambiguously determined from the experimental data.[39] The simplest solution of this problem is based on the irreversible Van Slyke-Cullen mechanism,[40] in which substrate binding occurs with an apparent bimolecular association constant that is described by the specificity constant, $k_N = k_2/K_m$. In other words, this approach provides the lowest value of k_1 of the Michaelis – Menten mechanism (Scheme 1).[39]

The biphasic kinetics of excision of the Sp and Gh lesions by NEIL1, as well as the inhibitory effect of XPC, can be summarized by the following steps:

This scheme represents the minimum number of steps, that can account for the experimental observations in Figures 4 and 5. The ratios of the kinetic parameters k_N and k_X can be estimated by numerical analysis of the kinetics of the reactions.[24, 39] According to this mechanism, the strand cleavage induced by NEIL1 is an irreversible bimolecular reaction that occurs with a rate proportional to the rate constant k_N. Our experiments showed that at NEIL1 concentrations of ~ 5 nM, the rate of cleavage occurs on a time scale faster than the experimental manual mixing time, τ_m~ 5 – 10 s. The lower limit of the value of k_N can be estimated as $k_N = 1/(\tau_m[NEIL1]_0)$ τ $(3 – 5)\times10^7$ $M^{-1}s^{-1}$. In turn, the upper limit is $k_N = k_2/[NEIL1]_0 \sim 5\times10^8$ $M^{-1}s^{-1}$ with $k_2 \sim 2 – 3$ s^{-1}, the experimentally measured values for Sp/Gh lesions.[12] If $k_N \geq 5\times10^8$ $M^{-1}s^{-1}$, the reaction rate-limiting step will controlled by the first order rate constant, k_2. The recycling step (rate constant k_3) can be excluded from

Scheme 1 because the denaturing gel assays provide a measure of the total concentrations of incision products (P = dissociated + undissociated NEIL1-P complexes).

The gradual reduction of the burst phase amplitude as a function of increasing XPC concentration in Figure 4 indicates that the formation of XPC-HDNA complexes competes with the binding of NEIL1 and the subsequent strand cleavage reaction (Scheme 2). Under single turnover conditions, the effect of XPC concentration on the reciprocal burst phase amplitude can be expressed by the following equation,

$$1/A_b = 1 + (k_X/k_N)([XPC]_0/[NEIL1]_0) \quad (1)$$

where A_b is the burst phase amplitude estimated by a linear extrapolation of the data points of the slow kinetic phase to the t = 0 time point (Figures 4 and 5); $[NEIL1]_0$ and $[XPC]_0$ are the total protein concentrations (Figure 4). Equation 1 predicts that the value of $1/A_b$ should increase linearly as a function of the $[XPC]_0/[NEIL1]_0$ ratio. The experimental results shown in Figure 6 are consistent with this prediction and the slope yields the ratio k_X/k_N = 0.81±0.04.

This value is in very good agreement with the results obtained by the analysis of the NEIL1 incision kinetics by the DynaFit4 program (Table 1).

The slow kinetic phase of product formation is controlled by the dissociation of the XPC-HDNA complex (k_{-X}) followed by the prompt and irreversible strand cleavage reaction under single turnover conditions. The value of k_{-X} was obtained from the numerical analysis of the experimental kinetic data using the DynaFit4 program.[24, 39] The numerical values of k_{-X} and k_X/k_N thus are consistent with the model (Scheme 2) and the experimental data. In this analysis, a constant value of $k_N = 1\times10^8$ $M^{-1}s^{-1}$ was assumed that is consistent with diffusion-controlled bimolecular association rate constants ($10^8 - 10^9$ $M^{-1}s^{-1}$).[39, 41] The time course of the incision reactions calculated by the DynaFit4 program using the indicated kinetic parameters provide a good fit to the experimental data points (Figures 4B,C and 5). We note that variations of k_N within the range of 3×10^7 to 3×10^8 $M^{-1}s^{-1}$, reduces the characteristic rise time of the burst phase, but does not affect the value of k_X (Figure S3 in Supporting Information). Numeric analysis of the kinetic data suggests that complexes of XPC with SpDNA are somewhat more stable than complexes with GhDNA since the rate constant, k_{-X} for SpDNA is ~ 3 times smaller than in the case of GhDNA.

Effects of Nonspecific Competitor DNA on the Excision of Gh and Sp DNA Lesions by NEIL1

In cells, the repair of DNA lesions occurs in the context of genomic DNA. NEIL1 is known to bind non-specifically to unmodified DNA that reduces its efficiency to excise DNA lesion substrates.[42] The effects of unmodified 147-mer DNA duplexes (umDNA) on NEIL1 – catalyzed excision of hydantoin lesions are shown in Figure 7.

Figure 7 shows that in the presence of an excess of umDNA, the amplitude of the burst phase associated with the NEIL1-induced incision of GhDNA duplexes is gradually reduced to ~ 10% as the $[umDNA]_0/[NEIL1]_0$ ratio is increased. Furthermore, the burst phase is

followed by a slower time-resolved kinetic component as in the case of the XPC competitor experiments (Figure 4).

The biphasic kinetics observed in the presence of umDNA can be described by Scheme 3.

In this scheme, H = Gh, and the inhibition effect of umDNA is described by three kinetic parameters (k_N, k_{umD}, and k_{-umD}) that is similar to Scheme 2 that describes the inhibition of NEIL1 incision activity by XPC-RAD23B.

Figure 8 shows that the reciprocal burst phase amplitude increases linearly with increasing $[umDNA]_0/[NEIL1]_0$ ratios ≥ 1.5 that is consistent with the equation

$$1/A_b = 1 + (k_{um}/k_N)([umDNA]_0/[NEIL1]_0) \quad (2)$$

which is similar to eq. 1 for the inhibition effect of XPC-RAD23B. The ratio k_{umD}/k_N = 0.95±0.05 at $[umDNA]_0/[NEIL1]_0$ ≥ 1.5 was determined from the slope of the linear portion of the plot shown in Figure 8.

At $[umDNA]_0/[NEIL1]_0$ ratios < 1, in agreement with experiment, the DynaFit4 analysis according to Scheme 3, predicts that the dependence of $1/A_b$ vs $[umDNA]_0/[NEIL1]_0$ is nonlinear at low umDNA concentrations because the small changes in NEIL1 concentraions are insufficient to substantially affect the magnitude of the burst phase (solid line in Figure 8). By contrast, the inhibition of NEIL1-catalyzed strand cleavage by XPC-RAD23B is linear at all values of [XPC] >>0 (Figure 6) as predicted by eq. 1. In turn, at $[umDNA]_0/[NEIL1]_0$ ratios >> 1 the slope of the $1/A_b$ vs $[umDNA]_0/[NEIL1]_0$ plots predicted by Scheme 3 is proportional to k_{um}/k_N ratio (Figure S4, Supporting Information).

Further analysis of the inhibitory effect of unmodified DNA on the BER activity of NEIL1 was performed using the DynaFit4 software. In summary, the averaged values of the parameters obtained in six independent experiments using DynaFit4 are the following: k_{umD}/k_N = 0.98±0.15, and the dissociation rate constant of NEIL1-umDNA complexes is k_{-umD} = (7.8±0.9)×10^{-4} s^-. Thus, the binding of NEIL1 to duplexes containing hydantoins lesions or to unmodified DNA duplexes occurs with similar rate constants. A similar effect has been reported for *EcoRV* restriction endonucleases that bind with the identical association rate constants to DNA molecules that either contained or lacked the *EcoRV* recognition sites.[43, 44]

CONCLUSIONS AND PERSPECTIVES

Monitoring the glycosylase/lyase activity of the bifunctional DNA glycosylase NEIL1 we have demonstrated that the DNA damage-sensing NER factor XPC reduces the rates of incisions of the double-stranded DNA substrates containing the hydantoin Gh or Sp lesions. Numerical analysis of the kinetic data indicates that both NEIL1 and XPC proteins bind rapidly to the GhDNA or SpDNA substrates with rate constants close to the diffusion limit for bimolecular association rate constants of other proteins.[39, 41] Thus, the preliminary partitioning of binding of NEIL1 and XPC to Gh/SpDNA hydantoin DNA lesions is determined by free diffusion mechanisms. The lifetimes of XPC-RAD23B complexes

calculated from the dissociation constants (Table 1) ~6 min (GhDNA) and ~19 min (SpDNA). In comparison, the lifetimes of XPC-RAD23B complexes with UV-damaged DNA obtained by EMSA methods are 20 – 30 min.[45] We conclude that, at cellular levels, similar competitive processes between the NER XPC and BER NEIL1 proteins may play a role in the 5 – 10 times more efficient repair of hydantoin lesions by BER than by NER mechanisms in intact cells.[22] In addition, the competing non-specific binding of XPC and NEIL1 to DNA lesions in intact cells significantly diminishes their removal by both NER and BER mechanisms and explains why high concentrations of these proteins are found in human cells. In human mesothelial cells, the nuclear concentrations of NEIL1 are in the range of 250 – 800 nM,[42, 46] while the concentrations of XPC in human fibroblasts were reported to be 140 nM.[47]

In the chromatin environment of human cells, access of the DNA to repair proteins is hindered, and thus the efficiencies of NER and BER mechanisms are reduced.[48, 49] It has been shown that in nucleosomes, the efficiency of NER in human cell extracts is significantly lower than in the case of free DNA.[32, 50] In general, BER proteins are smaller in size than the NER-initiating factor XPC-RAD23B, but BER excision activities are also reduced in nucleosomes.[42] Furthermore, chromatin remodelling factors can lead to an enhancement of NER and BER activities in intact cells that facilitate access of the DNA lesions to proteins of both pathways.[51] Finally, it has been shown that centrin-2 binds to XPC and enhances NER dual incision activities of UV photolesions in cell-free extracts.[52, 53] It remains to be seen whether the BER-NER protein binding competition reported here in vitro for oxidatively generated guanine lesions, will also be observable in the more complex environments of human cells.

Supplementary Material

Refer to Web version on PubMed Central for supplementary material.

ACKNOWLEDGMENTS

We are most grateful to Steven R. Lloyd who generously provided the NEIL1 protein.

Funding

This work was supported by the National Institute of Environmental Health Sciences grant R01 ES-027059 to V.S.

ABBREVIATIONS

BER	base excision repair
NER	nucleotide excision repair
8-oxoG	8-oxo-7,8-dihydroguanine Gh, 5-guanidinohydantoin
Sp	spiroiminodihydantoin
bp	base pair
EMSA	electrophoretic mobility shift assay

PAGE polyacrylamide gel electrophoresis

REFERENCES

[1]. Scott TL, Rangaswamy S, Wicker CA, and Izumi T (2014) Repair of oxidative DNA damage and cancer: recent progress in DNA base excision repair, Antioxid. Redox Signal. 20, 708–726. [PubMed: 23901781]

[2]. Lindahl T, and Wood RD (1999) Quality control by DNA repair, Science 286, 1897–1905. [PubMed: 10583946]

[3]. Wallace SS (2014) Base excision repair: a critical player in many games, DNA Repair (Amst) 19, 14–26. [PubMed: 24780558]

[4]. Marteijn JA, Lans H, Vermeulen W, and Hoeijmakers JH (2014) Understanding nucleotide excision repair and its roles in cancer and ageing, Nat. Rev. Mol. Cell. Biol. 15, 465–481. [PubMed: 24954209]

[5]. Yu Y, Cui Y, Niedernhofer LJ, and Wang Y (2016) Occurrence, Biological Consequences, and Human Health Relevance of Oxidative Stress-Induced DNA Damage, Chem. Res. Toxicol. 29, 2008–2039. [PubMed: 27989142]

[6]. Cadet J, Douki T, and Ravanat JL (2008) Oxidatively generated damage to the guanine moiety of DNA: mechanistic aspects and formation in cells, Acc. Chem. Res. 41, 1075–1083. [PubMed: 18666785]

[7]. Steenken S, and Jovanovic SV (1997) How easily oxidizable is DNA? One-electron reduction potentials of adenosine and guanosine radicals in aqueous solution, J. Am. Chem. Soc. 119, 617–618.

[8]. Fleming AM, Muller JG, Dlouhy AC, and Burrows CJ (2012) Structural context effects in the oxidation of 8-oxo-7,8-dihydro-2'-deoxyguanosine to hydantoin products: electrostatics, base stacking, and base pairing, J. Am. Chem. Soc. 134, 15091–15102. [PubMed: 22880947]

[9]. Mangerich A, Knutson CG, Parry NM, Muthupalani S, Ye W, Prestwich E, Cui L, McFaline JL, Mobley M, Ge Z, Taghizadeh K, Wishnok JS, Wogan GN, Fox JG, Tannenbaum SR, and Dedon PC (2012) Infection-induced colitis in mice causes dynamic and tissue-specific changes in stress response and DNA damage leading to colon cancer, Proc. Natl. Acad. Sci. U.S.A. 109, E1820–E1829. [PubMed: 22689960]

[10]. Henderson PT, Delaney JC, Muller JG, Neeley WL, Tannenbaum SR, Burrows CJ, and Essigmann JM (2003) The hydantoin lesions formed from oxidation of 7,8-dihydro-8-oxoguanine are potent sources of replication errors in vivo, Biochemistry 42, 9257–9262. [PubMed: 12899611]

[11]. Hailer MK, Slade PG, Martin BD, Rosenquist TA, and Sugden KD (2005) Recognition of the oxidized lesions spiroiminodihydantoin and guanidinohydantoin in DNA by the mammalian base excision repair glycosylases NEIL1 and NEIL2, DNA Repair (Amst) 4, 41–50. [PubMed: 15533836]

[12]. Krishnamurthy N, Zhao X, Burrows CJ, and David SS (2008) Superior removal of hydantoin lesions relative to other oxidized bases by the human DNA glycosylase hNEIL1, Biochemistry 47, 7137–7146. [PubMed: 18543945]

[13]. Zhao X, Krishnamurthy N, Burrows CJ, and David SS (2010) Mutation versus repair: NEIL1 removal of hydantoin lesions in single-stranded, bulge, bubble, and duplex DNA contexts, Biochemistry 49, 1658–1666. [PubMed: 20099873]

[14]. Krokeide SZ, Laerdahl JK, Salah M, Luna L, Cederkvist FH, Fleming AM, Burrows CJ, Dalhus B, and Bjoras M (2013) Human NEIL3 is mainly a monofunctional DNA glycosylase removing spiroimindiohydantoin and guanidinohydantoin, DNA Repair (Amst) 12, 1159–1164. [PubMed: 23755964]

[15]. Bandaru V, Sunkara S, Wallace SS, and Bond JP (2002) A novel human DNA glycosylase that removes oxidative DNA damage and is homologous to Escherichia coli endonuclease VIII, DNA Repair (Amst) 1, 517–529. [PubMed: 12509226]

[16]. Morland I, Rolseth V, Luna L, Rognes T, Bjoras M, and Seeberg E (2002) Human DNA glycosylases of the bacterial Fpg/MutM superfamily: an alternative pathway for the repair of 8-

oxoguanine and other oxidation products in DNA, Nucleic Acids Res. 30, 4926–4936. [PubMed: 12433996]

[17]. Hazra TK, Izumi T, Boldogh I, Imhoff B, Kow YW, Jaruga P, Dizdaroglu M, and Mitra S (2002) Identification and characterization of a human DNA glycosylase for repair of modified bases in oxidatively damaged DNA, Proc. Natl. Acad. Sci. U.S.A. 99, 3523–3528. [PubMed: 11904416]

[18]. Melis JP, van Steeg H, and Luijten M (2013) Oxidative DNA damage and nucleotide excision repair, Antioxid. Redox Signal. 18, 2409–2419. [PubMed: 23216312]

[19]. Lee TH, and Kang TH (2019) DNA Oxidation and Excision Repair Pathways, Int. J. Mol. Sci. 20, 6092–6092.

[20]. de Melo JT, de Souza Timoteo AR, Lajus TB, Brandao JA, de Souza-Pinto NC, Menck CF, Campalans A, Radicella JP, Vessoni AT, Muotri AR, and Agnez-Lima LF (2016) XPC deficiency is related to APE1 and OGG1 expression and function, Mutat. Res. 784–785, 25–33.

[21]. Shafirovich V, Kropachev K, Anderson T, Liu Z, Kolbanovskiy M, Martin BD, Sugden K, Shim Y, Chen X, Min JH, and Geacintov NE (2016) Base and Nucleotide Excision Repair of Oxidatively Generated Guanine Lesions in DNA, J. Biol. Chem. 291, 5309–5319. [PubMed: 26733197]

[22]. Shafirovich V, Kropachev K, Kolbanovskiy M, and Geacintov NE (2019) Excision of Oxidatively Generated Guanine Lesions by Competing Base and Nucleotide Excision Repair Mechanisms in Human Cells, Chem. Res. Tox. 32, 753–761.

[23]. Fried M, and Crothers DM (1981) Equilibria and kinetics of lac repressor-operator interactions by polyacrylamide gel electrophoresis, Nucleic Acids Res. 9, 6505–6525. [PubMed: 6275366]

[24]. Kuzmic P (1996) Program DYNAFIT for the analysis of enzyme kinetic data: application to HIV proteinase, Anal. Biochem. 237, 260–273. [PubMed: 8660575]

[25]. Joffe A, Geacintov NE, and Shafirovich V (2003) DNA lesions derived from the site-selective oxidation of guanine by carbonate radical anions, Chem. Res. Toxicol. 16, 1528–1538. [PubMed: 14680366]

[26]. Crean C, Uvaydov Y, Geacintov NE, and Shafirovich V (2008) Oxidation of single-stranded oligonucleotides by carbonate radical anions: generating intrastrand cross-links between guanine and thymine bases separated by cytosines, Nucleic Acids Res. 36, 742–755. [PubMed: 18084033]

[27]. Rokhlenko Y, Geacintov NE, and Shafirovich V (2012) Lifetimes and reaction pathways of guanine radical cations and neutral guanine radicals in an oligonucleotide in aqueous solutions, J. Am. Chem. Soc. 134, 4955–4962. [PubMed: 22329445]

[28]. Kornyushyna O, Berges AM, Muller JG, and Burrows CJ (2002) In vitro nucleotide misinsertion opposite the oxidized guanosine lesions spiroiminodihydantoin and guanidinohydantoin and DNA synthesis past the lesions using Escherichia coli DNA polymerase I (Klenow fragment), Biochemistry 41, 15304–15314. [PubMed: 12484769]

[29]. Khutsishvili I, Zhang N, Marky LA, Crean C, Patel DJ, Geacintov NE, and Shafirovich V (2013) Thermodynamic profiles and nuclear magnetic resonance studies of oligonucleotide duplexes containing single diastereomeric spiroiminodihydantoin lesions, Biochemistry 52, 1354–1363. [PubMed: 23360616]

[30]. Fleming AM, Orendt AM, He Y, Zhu J, Dukor RK, and Burrows CJ (2013) Reconciliation of chemical, enzymatic, spectroscopic and computational data to assign the absolute configuration of the DNA base lesion spiroiminodihydantoin, J. Am. Chem. Soc. 135, 18191–18204. [PubMed: 24215588]

[31]. Lowary PT, and Widom J (1998) New DNA sequence rules for high affinity binding to histone octamer and sequence-directed nucleosome positioning, J. Mol. Biol. 276, 19–42. [PubMed: 9514715]

[32]. Shafirovich V, Kolbanovskiy M, Kropachev K, Liu Z, Cai Y, Terzidis MA, Masi A, Chatgilialoglu C, Amin S, Dadali A, Broyde S, and Geacintov NE (2019) Nucleotide excision repair and impact of site-specific 5′,8-cyclopurine and bulky DNA lesions on the physical properties of nucleosomes, Biochemistry 58, 561–574. [PubMed: 30570250]

[33]. Roy LM, Jaruga P, Wood TG, McCullough AK, Dizdaroglu M, and Lloyd RS (2007) Human polymorphic variants of the NEIL1 DNA glycosylase, J. Biol. Chem. 282, 15790–15798. [PubMed: 17389588]

[34]. Lee YC, Cai Y, Mu H, Broyde S, Amin S, Chen X, Min JH, and Geacintov NE (2014) The relationships between XPC binding to conformationally diverse DNA adducts and their excision by the human NER system: Is there a correlation?, DNA Repair (Amst) 19, 55–63. [PubMed: 24784728]

[35]. Porello SL, Leyes AE, and David SS (1998) Single-turnover and pre-steady-state kinetics of the reaction of the adenine glycosylase MutY with mismatch-containing DNA substrates, Biochemistry 37, 14756–14764. [PubMed: 9778350]

[36]. Sugasawa K, Okamoto T, Shimizu Y, Masutani C, Iwai S, and Hanaoka F (2001) A multistep damage recognition mechanism for global genomic nucleotide excision repair, Genes Dev. 15, 507–521. [PubMed: 11238373]

[37]. Dou H, Mitra S, and Hazra TK (2003) Repair of oxidized bases in DNA bubble structures by human DNA glycosylases NEIL1 and NEIL2, J. Biol. Chem. 278, 49679–49684. [PubMed: 14522990]

[38]. Adamson NJ, and Reynolds EC (1997) Rules relating electrophoretic mobility, charge and molecular size of peptides and proteins, J. Chromatogr. B: Biomed. Sci. Appl. 699, 133–147. [PubMed: 9392373]

[39]. Kuzmic P (2009) Application of the Van Slyke-Cullen irreversible mechanism in the analysis of enzymatic progress curves, Anal. Biochem. 394, 287–289. [PubMed: 19627979]

[40]. Van Slyke DD, and Cullen GE (1914) The mode of action of urease and of enzymes in general, J. Biol. Chem. 19, 141–180.

[41]. Halford SE (2009) An end to 40 years of mistakes in DNA-protein association kinetics?, Biochem. Soc. Trans. 37, 343–348. [PubMed: 19290859]

[42]. Odell ID, Newick K, Heintz NH, Wallace SS, and Pederson DS (2010) Non-specific DNA binding interferes with the efficient excision of oxidative lesions from chromatin by the human DNA glycosylase, NEIL1, DNA Repair (Amst) 9, 134–143. [PubMed: 20005182]

[43]. Taylor JD, Badcoe IG, Clarke AR, and Halford SE (1991) EcoRV restriction endonuclease binds all DNA sequences with equal affinity, Biochemistry 30, 8743–8753. [PubMed: 1909572]

[44]. Erskine SG, Baldwin GS, and Halford SE (1997) Rapid-reaction analysis of plasmid DNA cleavage by the EcoRV restriction endonuclease, Biochemistry 36, 7567–7576. [PubMed: 9200708]

[45]. Batty D, Rapic'-Otrin V, Levine AS, and Wood RD (2000) Stable binding of human XPC complex to irradiated DNA confers strong discrimination for damaged sites, J. Mol. Biol. 300, 275–290. [PubMed: 10873465]

[46]. Odell ID, Newick K, Heintz NH, Wallace SS, and Pederson DS (2010) Corrigendum to "Non-specific DNA binding interferes with the efficient excision of oxidative lesions from chromatin by the human DNA glycosylase, NEIL1" [DNA Repair 9 (2010) 134–143], *DNA* Repair (Amst) 9, 938–938.

[47]. Luijsterburg MS, von Bornstaedt G, Gourdin AM, Politi AZ, Mone MJ, Warmerdam DO, Goedhart J, Vermeulen W, van Driel R, and Hofer T (2010) Stochastic and reversible assembly of a multiprotein DNA repair complex ensures accurate target site recognition and efficient repair, J. Cell. Biol. 189, 445–463. [PubMed: 20439997]

[48]. Nag R, and Smerdon MJ (2009) Altering the chromatin landscape for nucleotide excision repair, Mutat. Res, doi:10.1016/j.mrrev.2009.1001.1002.

[49]. Rodriguez Y, Hinz JM, and Smerdon MJ (2015) Accessing DNA damage in chromatin: Preparing the chromatin landscape for base excision repair, DNA Repair (Amst) 32, 113–119. [PubMed: 25957487]

[50]. Hara R, Mo J, and Sancar A (2000) DNA damage in the nucleosome core is refractory to repair by human excision nuclease, Mol. Cell. Biol. 20, 9173–9181. [PubMed: 11094069]

[51]. Hara R, and Sancar A (2002) The SWI/SNF chromatin-remodeling factor stimulates repair by human excision nuclease in the mononucleosome core particle, Mol. Cell. Biol. 22, 6779–6787. [PubMed: 12215535]

[52]. Nishi R, Okuda Y, Watanabe E, Mori T, Iwai S, Masutani C, Sugasawa K, and Hanaoka F (2005) Centrin 2 stimulates nucleotide excision repair by interacting with xeroderma pigmentosum group C protein, Mol. Cell. Biol. 25, 5664–5674. [PubMed: 15964821]

[53]. Nishi R, Sakai W, Tone D, Hanaoka F, and Sugasawa K (2013) Structure-function analysis of the EF-hand protein centrin-2 for its intracellular localization and nucleotide excision repair, Nucleic Acids Res. 41, 6917–6929. [PubMed: 23716636]

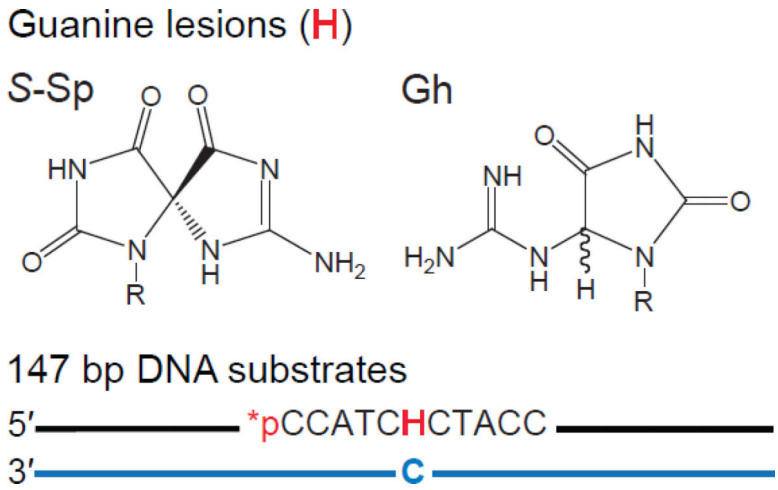

Figure 1.

Structure of the 147 bp ^{32}P-internally labeled (*p) double-stranded DNA substrates harboring site-specifically positioned guanine lesions (H = *S*-Sp, or Gh).

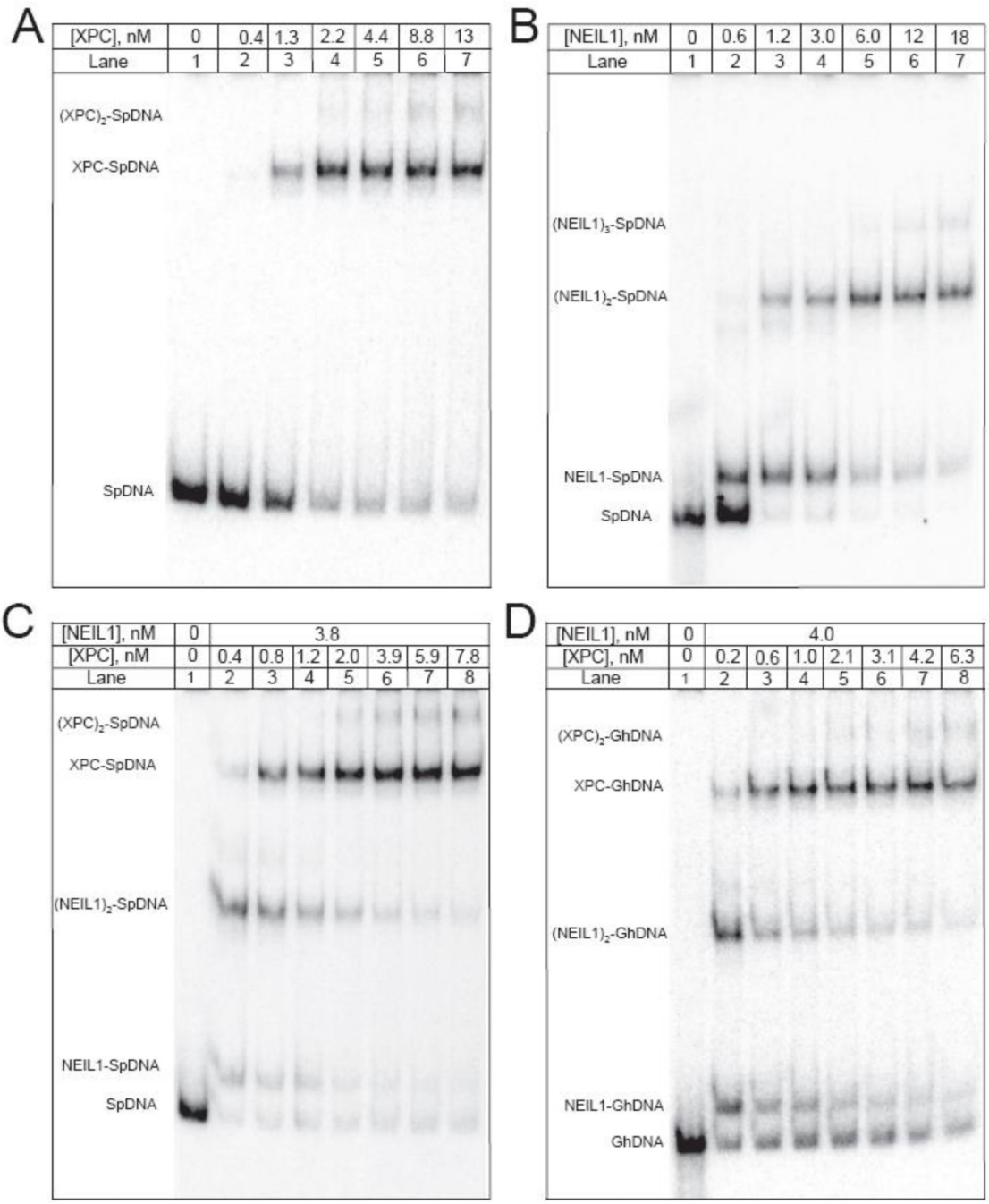

Figure 2.

Competitive binding of XPC-RAD23B and NEIL1 to single hydantoin lesions in double-stranded DNA to 147 bp ^{32}P-internally labeled SpDNA and GhDNA duplexes in the presence of nonspecific pBR322 DNA competitor. (A) Binding of XPC-RAD23B to SpDNA; (B) Binding of NEIL1 to SpDNA; competitive binding of the premixed NEIL1 and XPC-RAD23B to SpDNA (C) or GhDNA (D). [SpDNA] or [GhDNA] concentrations, 0.1 nM, [pBR322] concentration, 1.8 nM.

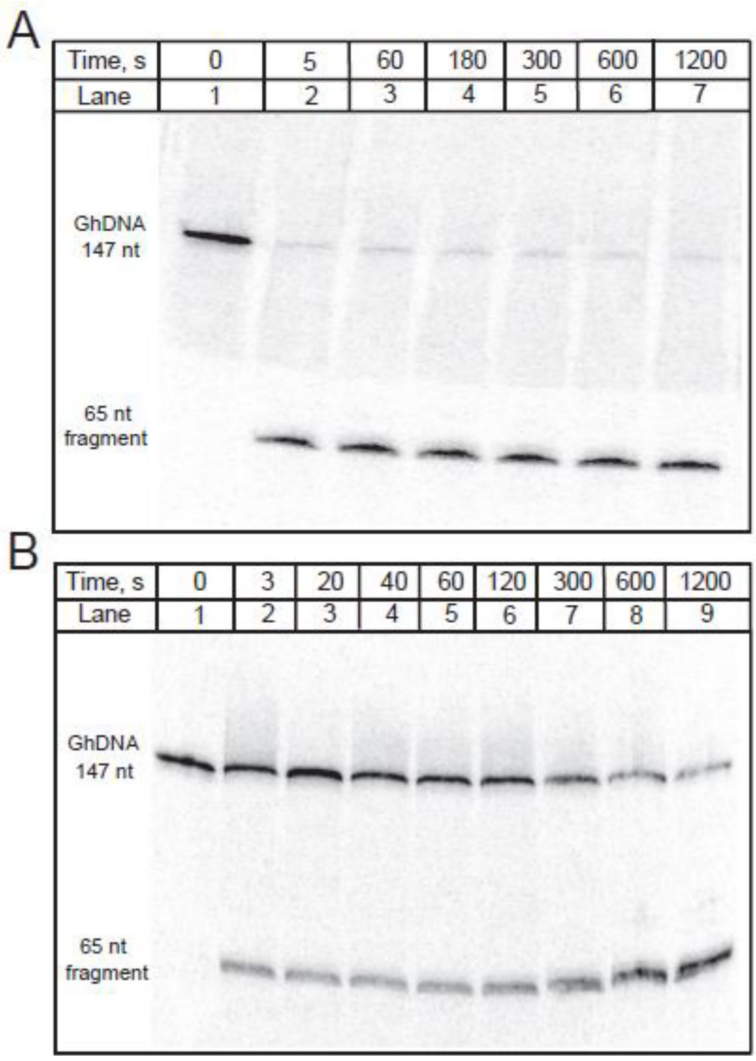

Figure 3.

Representative autoradiographs of denaturing gel assays of cleavage of 147 bp ^{32}P-internally labeled GhDNA duplexes (0.1 nM) induced by NEIL1 (5.8 nM) in the absence (A) or in the presence (B) of 4.5 nM XPC-RAD23B. Analogous results were obtained with SpDNA duplexes (data not shown).

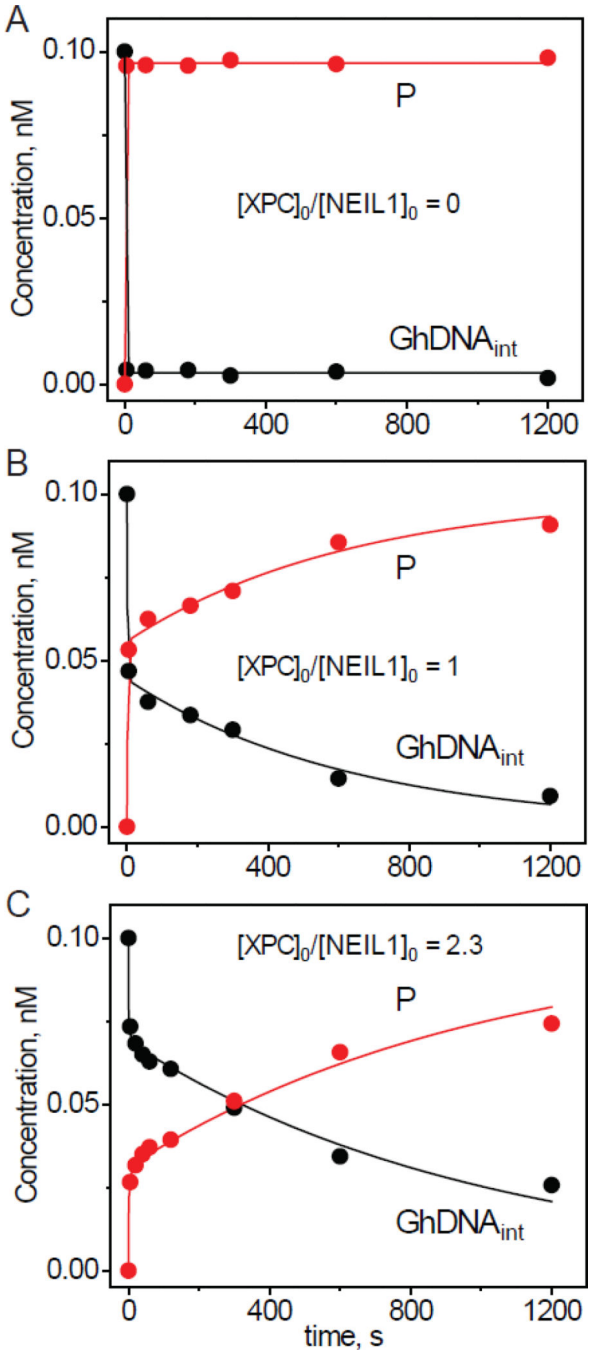

Figure 4.

Effect of XPC-RAD23B on the formation of incision cleavage products in 147 bp ^{32}P-internally labeled GhDNA duplexes (0.1 nM) at different ratios of [XPC]$_0$/[NEIL1]$_0$ proteins. (Averages of three independent experiments are shown). The data points (all error bars ≤ 10%) represent concentrations of total cleavage products [P] (arising from dissociated and undissociated NEIL1-Gh-DNA complexes) and intact DNA substrates, [GhDNA$_{int}$]. (A) [hNEIL1] = 5.8 nM, (B) 5.3 nM, and (C) 6.3 nM. All parameters are defined in Schemes 1 and 2 in the text. The solid lines represent the computed values of [P] and [GhDNA$_{int}$] =

[GhDNA] + [XPC-GhDNA] from numerical least-squares fits of the kinetic parameters (Scheme 2) to the experimental data points. Fixed parameters: $k_1 = 1\times10^8\ M^{-1}s^{-1}$; optimized parameters with standard errors representing 95% confidence intervals: k_X/k_N = 0.78±0.04 (B), and 0.94±0.5 (C); $k_{-X} = (2.8\pm0.3)\times10^{-3}\ s^{-1}$ (B), and $(3.2\pm0.3)\times10^{-3}\ s^{-1}$ (C).

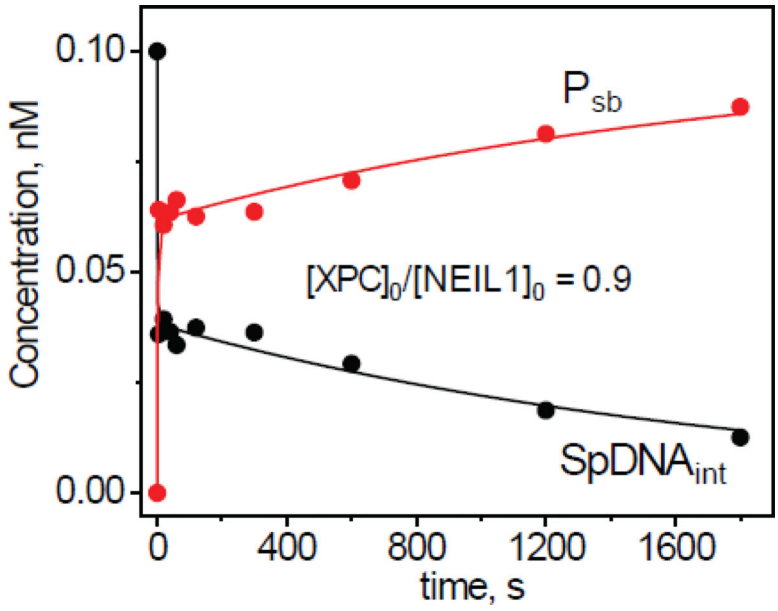

Figure 5.

Effect of XPC-RAD23B on BER incisions of 147 bp ^{32}P-internally labeled SpDNA duplexes (0.1 nM) induced by NEIL1 (5.2 nM). The data points represent the total concentrations of [P] and intact substrate, [$SpDNA_{int}$]; all error bars ≤ 10%). The solid lines represent the computed numerical least-squares fits of the kinetic parameters (Scheme 2) to the experimental data points. Fixed parameter $k_1 = 1\times10^8$ $M^{-1}s^{-1}$; optimized parameters (standard errors representing 95% confidence intervals): $k_X/k_N = 0.66\pm0.02$, $k_{-X} = (8.8\pm0.8)\times10^{-4}$ s^{-1}.

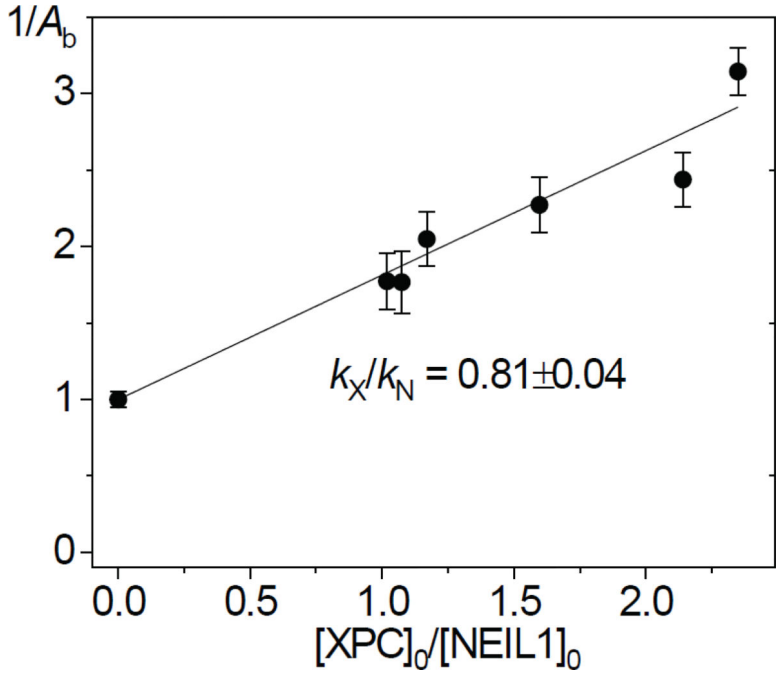

Figure 6.

Effect of XPC-RAD23B on the burst amplitude of the incisions induced by NEIL1 in 147 bp ^{32}P-internally labeled 5-guanidinohydantoin DNA duplexes (GhDNA, 0.1 nM). The solid line represents the numerical least-squares fit of the slope, $k_X/k_N = 0.81\pm0.04$ (eq 1) with standard errors representing 95% confidence intervals obtained in six independent experiments with the weighted standard errors shown by the error bars.

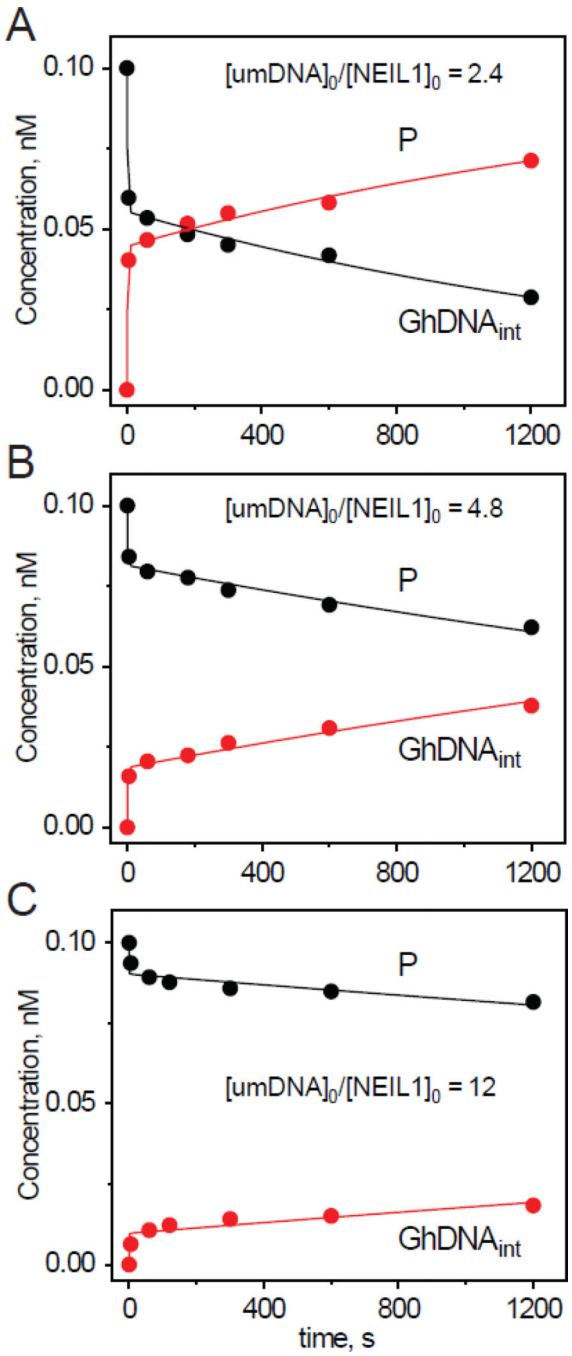

Figure 7.

Effect of different concentrations of 147 bp unmodified DNA duplexes (umDNA) on the formation of incisions of 147 bp ^{32}P-internally labeled GhDNA duplexes (0.1 nM) initiated by NEIL1 (4.2 nM). The data points (average values derived from three independent experiments; the error bars (≤ 10%) are not shown). Concentrations of cleaved products [P], and intact DNA duplexes [$GhDNA_{int}$] are shown. The solid lines represent numerical least-squares fits of the kinetic parameters (Scheme 3) to the experimental data points using k_1 = 1×10^8 $M^{-1}s^{-1}$ as a fixed parameter, and optimized parameters with standard errors

representing 95% confidence intervals: (A) k_{umD}/k_N = 0.91±0.02, (B) 1.14±0.05, and (C) 0.83±0.06 and (A) k_{-umD} = (7.1±0.6)×10^{-4} s^{-1}, (B) (10.0±0.1)×10^{-4} s^{-1}, and (C) (8.8±0.2) ×10^{-4} s^{-1}.

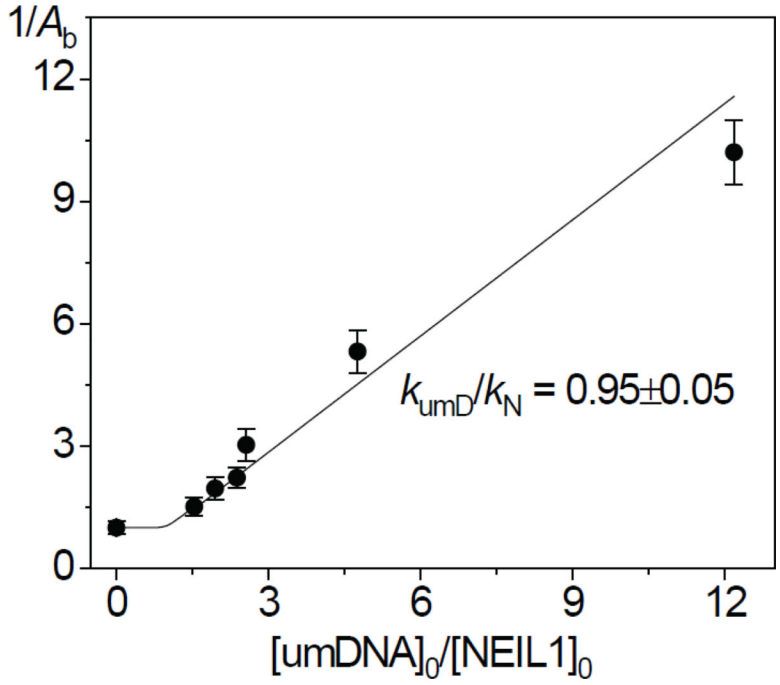

Figure 8.

Effect of umDNA on the burst amplitude of incisions induced by NEIL1 (4.2 nM) in 147 bp ^{32}P-internally labeled 5-guanidinohydantoin DNA duplexes (GhDNA, 0.1 nM). The solid line represents a numerical least-squares fit of eq. 2 to the experimental data points in the range $1.5 \leq [\text{umDNA}]_0/[\text{NEIL1}]_0 \leq 12$ (averages of six independent experiments) with $k_{\text{-umD}}/k_{\text{N}} = 0.95\pm0.05$; in the range $0 \leq [\text{umDNA}]_0/[\text{NEIL1}]_0 \leq 1.5$ the solid line was calculated using Dyanfit4 with [NEIL1] = 4.2 nM, $k_{\text{N}} = 1\times10^{8}$ $M^{-1}s^{-1}$, $k_{\text{umD}}/k_{\text{N}} = 0.95$ and $k_{\text{-umD}} = 1\times10^{-3}$ s^{-1} (Scheme 3).

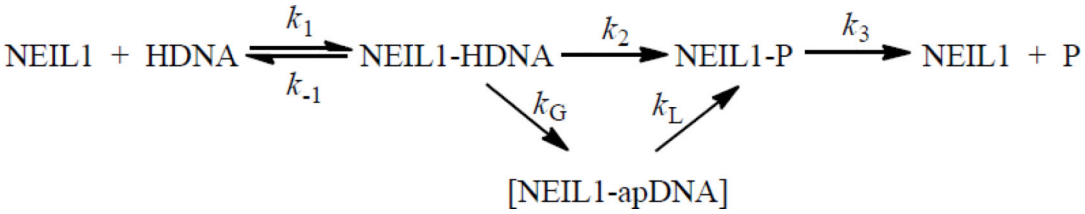

Scheme 1.

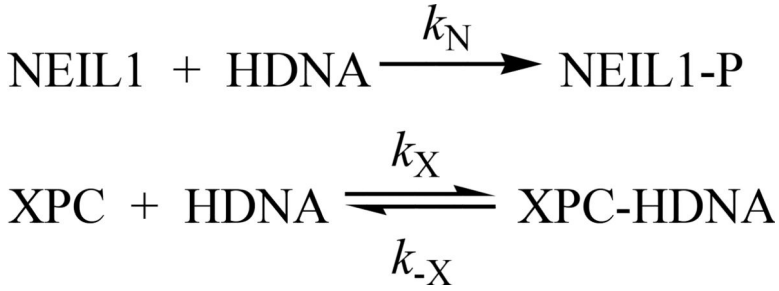

Scheme 2.

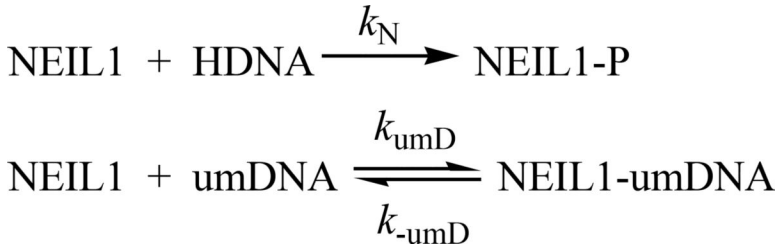

Scheme 3.

Table 1.

Kinetic parameters for reactions of XPC-RAD23B and hNEIL1 proteins with 147 bp double-stranded DNA substrates containing the NEIL1 substrates Sp and Gh according to Scheme 2.

DNA substrate	*k*X/*k*N	*k*-X, S^{-1}
GhDNA[a]	0.81±0.10	$(2.9\pm0.3)\times10^{-3}$
SpDNA[b]	0.66±0.02	$(8.8\pm0.8)\times10^{-4}$

Standard errors for data values obtained in six[a] or three[b] independent experiments represent 95% confidence intervals.